

Institutionen för systemteknik

Department of Electrical Engineering

Examensarbete

Starter Motor Protection

Examensarbete utfört i Fordonssystem
vid Tekniska högskolan i Linköping
av

Daniel Gerhardsson

LiTH-ISY-EX--10/4405--SE

Linköping 2010



Linköpings universitet
TEKNISKA HÖGSKOLAN

Starter Motor Protection

Examensarbete utfört i Fordonssystem
vid Tekniska högskolan i Linköping
av


Daniel Gerhardsson

LiTH-ISY-EX--10/4405--SE

Handledare: **Dr. Erik Geijer Lundin**
Scania CV AB
Ph.D. Student Christofer Sundström
ISY, Linköpings universitet

Examinator: **Assistant Professor Mattias Krysaner**
ISY, Linköpings universitet

Linköping, 31 March, 2010

	Avdelning, Institution Division, Department Division of Vehicular Systems Department of Electrical Engineering Linköpings universitet SE-581 83 Linköping, Sweden	Datum Date 2010-03-31
---	---	--

Språk Language <input type="checkbox"/> Svenska/Swedish <input checked="" type="checkbox"/> Engelska/English <input type="checkbox"/> _____	Rapporttyp Report category <input type="checkbox"/> Licentiatavhandling <input checked="" type="checkbox"/> Examensarbete <input type="checkbox"/> C-uppsats <input type="checkbox"/> D-uppsats <input type="checkbox"/> Övrig rapport <input type="checkbox"/> _____	ISBN _____ ISRN LiTH-isy-ex--10/4405--SE Serietitel och serienummer ISSN Title of series, numbering _____
--	---	---

URL för elektronisk version http://www.fs.isy.liu.se http://urn.kb.se/resolve?urn=urn:nbn:se:liu:diva-ZZZZ	
--	--

Titel Title	Startmotorskydd Starter Motor Protection
Författare Author	Daniel Gerhardsson

Sammanfattning
Abstract

Starter motors are sensitive for overheating. By estimating the temperature and preventing cranking in time, there is an option to avoid the dangerous temperatures. The truck manufacturer Scania CV AB proposed a master thesis that should evaluate the need of an overheating protection for the starter motor.

The aim is to evaluate any positive effects of implementing an algorithm that can estimate the brush temperature instead of using the available time constrain, which allows 35 seconds of cranking with a following 2 seconds delay, allowing the crank shaft to stop before a new start attempt is allowed. To achieve high load on the starter motor and high temperature in the brushes, tests were performed under -20° Celsius.

Initial testing on truck, under normal temperatures, showed that the batteries could not run the starter motor long enough to reach high temperatures in the brushes. This is believed to be caused by the voltage drop between the batteries and the starter motor, causing the starter motor to run in an operating area it is not optimized for. There are several other problems which gives a higher load on the engine, for example oil viscosity, resulting in higher currents, but those are not mentioned in this report.

Three different models are compared, Two State Model, Single State Model and a Time Constrained Model. Tests and verifications show that the Two State Model is superior when it comes to protecting the starter motor from overheating and at the same time maximizing the cranking time. The major difference between the Two State Model and the Single State Model are the cooling characteristics. In the Single State Model the brush temperature drops quickly to the outside temperature while in the Two State Model the brush temperature drops to a second state temperature instead of the outside temperature. With the currently implemented time constrain it is possible to overheat the starter motor. The algorithms are optimized under cold conditions, due to problems in reaching high temperatures under warmer conditions.

Nyckelord Keywords	
------------------------------	--

Abstract

Starter motors are sensitive for overheating. By estimating the temperature and preventing cranking in time, there is an option to avoid the dangerous temperatures. The truck manufacturer Scania CV AB proposed a master thesis that should evaluate the need of an overheating protection for the starter motor.

The aim is to evaluate any positive effects of implementing an algorithm that can estimate the brush temperature instead of using the available time constrain, which allows 35 seconds of cranking with a following 2 seconds delay, allowing the crank shaft to stop before a new start attempt is allowed. To achieve high load on the starter motor and high temperature in the brushes, tests were performed under -20° Celsius.

Initial testing on truck, under normal temperatures, showed that the batteries could not run the starter motor long enough to reach high temperatures in the brushes. This is believed to be caused by the voltage drop between the batteries and the starter motor, causing the starter motor to run in an operating area it is not optimized for. There are several other problems which gives a higher load on the engine, for example oil viscosity, resulting in higher currents, but those are not mentioned in this report.

Three different models are compared, Two State Model, Single State Model and a Time Constrained Model. Tests and verifications show that the Two State Model is superior when it comes to protecting the starter motor from overheating and at the same time maximizing the cranking time. The major difference between the Two State Model and the Single State Model are the cooling characteristics. In the Single State Model the brush temperature drops quickly to the outside temperature while in the Two State Model the brush temperature drops to a second state temperature instead of the outside temperature. With the currently implemented time constrain it is possible to overheat the starter motor. The algorithms are optimized under cold conditions, due to problems in reaching high temperatures under warmer conditions.

Acknowledgments

I would like to thank my supervisor at Scania, Dr. Erik Geijer Lundin, for all his support and strong efforts during this thesis, not just as a supervisor, but also as a friend. For all useful feedback during this thesis, I would like to thank Assistant Professor Mattias Krysanter and Ph.D. Student Christofer Sundström at Linköping University. My group at Scania, NESX, deserves my respect for making me feel welcome and as a part of the group during my thesis.

A special thanks to my family, Andreas, Elin, Elsie, Emelie, Emilia, Erik, Fadila, Hamzalija, Ida, Lasse, Lena, Matilda, Mats, Monica and Nerima, for your unconditional love and support through my life.

Finally I would like to thank the love of my life, Ines, for being my role model and always showing faith in me. You are my better half, I love you.

Contents

1	Introduction	1
1.1	Background	1
1.2	Project Description	1
1.3	Competitor Analysis	2
1.4	Thesis outline	2
2	Theory	3
2.1	DC Motor	4
2.1.1	Series Wound Motor	5
2.2	Introduction To Heat Transfer	8
2.2.1	Temperature and Heat Flow	8
2.2.2	Heat Transfer Modes	8
3	Modeling	11
3.1	Physical Description	11
3.2	Warm Up	14
3.3	Parameter Calibrations	14
4	Results and Discussion	17
4.1	Testing and Verification	17
4.1.1	Complete Test on Truck	18
4.1.2	Time Constrained Model	21
4.1.3	Single State Model	21
4.1.4	Two State Model	22
4.1.5	Waiting Time Estimation	23
4.2	Discussion	26
5	Conclusions and Future Work	29
5.1	Conclusions	29
5.2	Future Work	29
	Bibliography	31

A	Appendix	33
A.1	Time Estimation	33
A.2	Zoomed Plots	35

Chapter 1

Introduction

In today's globalization, cutting cost and increasing effectiveness have become the primer goals for western based companies, especially during financially challenging times. Due to warranties, components and systems should last at least through the warranty period. If not succeeded, costs increase and primarily damage the reputation among customers. One of today's largest warranty issues in the truck industry is the starter motor. Starter motors are very expensive, sometimes mis-used and often become a warranty issue.

1.1 Background

If a truck does not start and there is a mistreat of the starter motor, there can be a number of different background causes, such as for example air in the fuel system. The misuse of the starter motor can be reduced by locating and eliminating these causes. To find and eliminate these causes can take up to several years, raising the importance of fast implementation of an overheating protection for the starter motor. A quick first step is to implement a fixed time constrain for cranking, which gives a fairly good protection, but is not a sustainable solution. This is the currently implemented solution (System developer Erik Geijer Lundin, Scania Meeting, 14.10.2009). A second step is to make an algorithm for heat estimation, which should give the starter motor sufficient protection against overheating.

1.2 Project Description

This thesis aims to construct an algorithm for overheating protection in a starter motor. Three different software approaches are focused upon. A Time Constrained Model, a Single State Model and a Multiple State Model. All three solutions use only current available hardware. When overheating occurs, a warning message should be presented through the driver interface with an estimated waiting time until next start is allowed. The result of this work will present a comparison of the obtained performance gain between the different solutions.

1.3 Competitor Analysis

A short glance on how Scania's competitors deal with overheating protection follows below. The study shows that Volvo currently is the only competitor which uses a complex algorithm for overheating protection.

Volvo

Volvo uses an automatic overheating protection model in both their D12 and D13 engines. The algorithm shuts down the start motor when overheating occurs and the cooling time is presented in the driver display for the D13 engine. There is no display presentation in the D12 engine [12].

MAN

MAN does not have an implementation of an overheating protection model. The driver's manual presents how to use the starter motor. It is stated that the maximum allowed runtime is 10 seconds with a 30 seconds cooling time [7].

Mercedes

Mercedes has a similar system as MAN. Maximum allowed runtime is 20 seconds with a 60 seconds cooling time. A cooling time of 3 minutes is recommended after three starting attempts [8].

1.4 Thesis outline

Chapter 2 will go into theory for DC models, especially Series Wound DC Motors, while Chapter 3 explains the model used to calculate the motor temperature. Chapter 4 contains results and discussion. Finally, Chapter 5 consists of conclusions and possible future work.

Chapter 2

Theory

In this chapter a background for DC motors is presented. A model for the Series Wound DC Motor is presented with the relations between torque, current, speed and voltage. In the last section of the chapter, theory of heat transfer is presented. Electric motors may be divided into two classic subgroups, DC and AC motors. An additional group is the universal motors, that consists of DC motors running on AC power. For the classification of electric motors, see Figure 2.1 [3]. Further attention is only paid to series wound motors in this report.

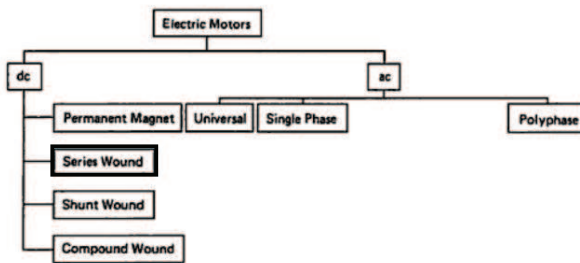


Figure 2.1. Classification of electric motors. In this thesis only Series Wound DC Motors are studied.

2.1 DC Motor

The first electric motor, using a commutator, was invented in 1832 by William Sturgeon. However, the principle of converting electric energy to mechanical energy was already shown in 1821 by Michael Faraday. Because there was no electrical distribution at the time and batteries were expensive, electric motors were no success. Not until 1886 the first practical DC motor was invented and in the following years, the DC motors was used in elevators, trolleys and subways [10]. The basic principle of a DC motor is shown in Figure 2.2. Applied current is

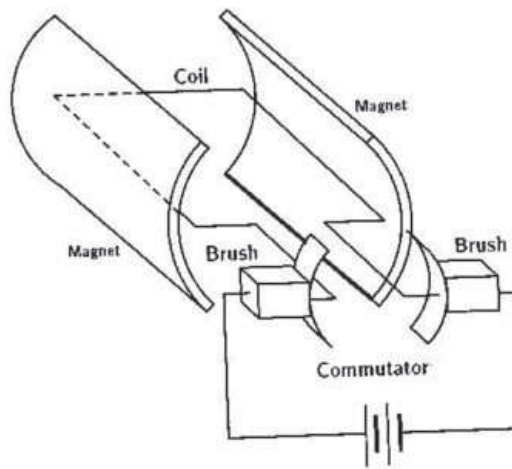


Figure 2.2. Principle of a DC motor. Current is transferred through the brushes to the coil which produces a magnetic field. The coil is then attracted to the magnets and starts to rotate. Every 180 degrees of change in the rotation, the current changes direction in the coil, thus changing the magnetic field.

transferred via brushes to a coil which produces a magnetic field. The coil rotates due to an attraction of another magnetic field produced by magnets. DC motors are often divided into four general subgroups: permanent magnet, shunt wound, series wound and compound wound DC motors. The torque to current relation between the subgroups is shown in Figure 2.3, that reveals why the series wound motor is used as starter motor. Series wound motors delivers high torque for lower armature current compared to the other options [1]. In series wound motors the field windings are connected in series with the armature and in shunt wound motors the field windings are connected in parallel with the armature. The electric starter motors used in todays trucks are series wound, which is why this report will be limited to the series wound motor.

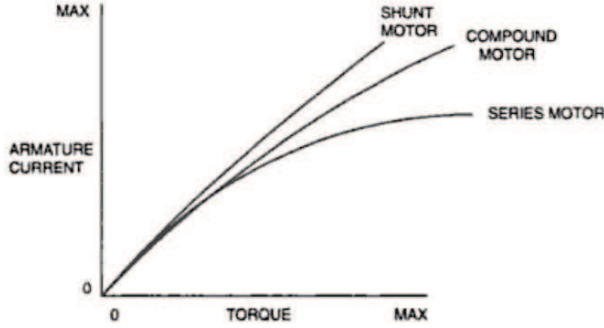


Figure 2.3. Torque versus current for the three subgroups of DC motors. The Series Motor produces higher torque for lower armature current compared to both shunt and compound motors, which makes it ideal as a starter motor [1].

2.1.1 Series Wound Motor

Series wound motors are superior when it comes to high starting torque and are therefore the electric motors used to start combustion engines. The principle of a series wound motor is shown in Figure 2.4. The basic parts are supply voltage V_T , the series field and the armature, where E_A is the armature voltage. A series

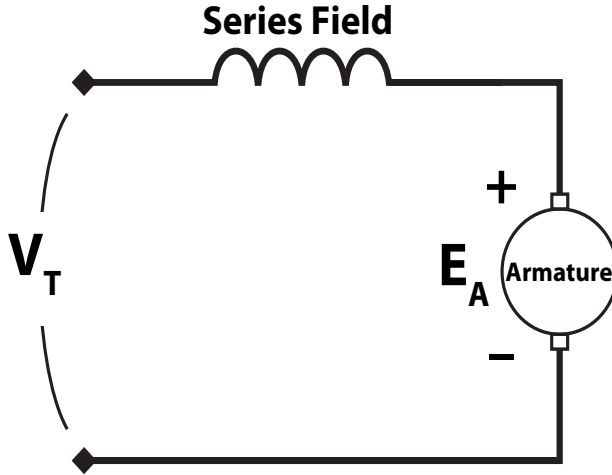


Figure 2.4. Simple model of a Series wound DC motor [1].

wound DC motor can be modeled by using a supplied voltage, field resistance, inductance and armature resistance [5]. Such a model is shown in Figure 2.5, where V_T is the supplied voltage, E_A the back electromotive force (back emf), I_A the armature current, L_F the field inductance, R_F the field resistance, R_A the armature windings and the brush resistance. The inductance L_F is in the

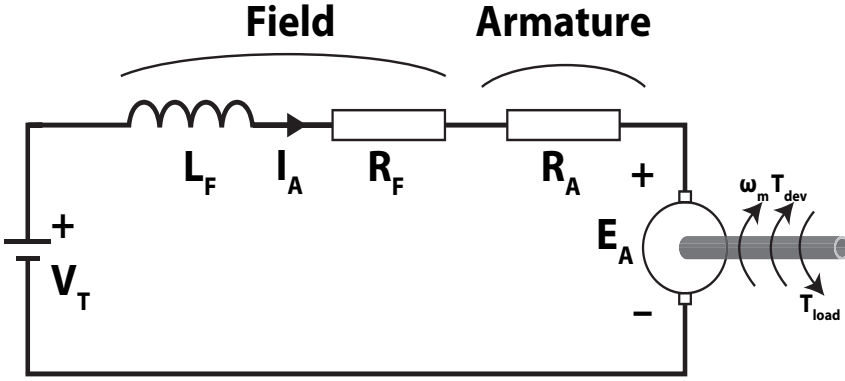


Figure 2.5. Series Wound DC Motor Circuit. Added to Figure 2.4 are the field and armature wire resistances.

following neglected since it behaves as a short circuit for DC currents. The back electromotive force, E_A , is the average voltage induced in the armature due to the motion of the conductors relative to the magnetic field and is given by

$$E_A = K\Phi\omega_m, \quad (2.1)$$

where K is the motor constant which depends on design parameters of the motor, Φ the magnetic flux and ω_m the angular velocity of the rotor. The developed torque is

$$T_{dev} = K\Phi I_A. \quad (2.2)$$

The developed mechanical power is

$$P_{dev} = \omega_m T_{dev}. \quad (2.3)$$

Another expression for the developed power is given by Joule's law [11],

$$P_{dev} = E_A I_A. \quad (2.4)$$

In a series wound DC motor the field current is the armature current, an equation for approximating Φ is therefore

$$\Phi = K_F I_A. \quad (2.5)$$

Here, K_F is a constant that depends on the number of field windings, the geometry of the magnetic circuit and the B-H characteristics of the iron. The relationship between Φ and I_A is nonlinear, due to the magnetic saturation of the iron B-H characteristics. Magnetic saturation is reached when an increase in external applied magnetizing field H cannot increase the magnetization of the iron further, which makes the magnetic field B to level off [5]. In this thesis the DC motor operates in a linear range, thus K_F is approximated with a constant. Using Equation (2.5) to substitute Φ in (2.1) yields

$$E_A = K K_F \omega_m I_A \quad (2.6)$$

and in Equation (2.2)

$$T_{dev} = K K_F I_A^2. \quad (2.7)$$

Applying Kirchoff's voltage law to Figure (2.5) yields an expression for the supply voltage,

$$V_T = (R_F + R_A) I_A + E_A, \quad (2.8)$$

and also with Equation (2.6),

$$V_T^2 = (R_F + R_A + K K_F \omega_m)^2 I_A^2.$$

Now to get an expression for the relationship between torque and speed for series wound motors, combine Equation (2.6) and (2.8) and replace the current in Equation (2.7),

$$T_{dev} = \frac{K K_F V_T^2}{(R_F + R_A + K K_F \omega_m)^2}.$$

Equations (2.4) and (2.6) are combined to get a new expression for the developed power,

$$P_{dev} = K K_F \omega_m I_A^2. \quad (2.9)$$

In order to find an expression for the power loss, an expression for input power is needed. The input power is a function of supply voltage and circuit current,

$$P_{in} = V_T I_A = (R_A + R_F + K K_F \omega_m) I_A^2. \quad (2.10)$$

Using Equation (2.9) and (2.10) ends up in an equation for the power loss,

$$P_{loss} = P_{in} - P_{dev} = (R_A + R_F) I_A^2. \quad (2.11)$$

In Chapter 3 a scaled version of Equation (2.11) is used for modeling the temperature increase of the brushes. Another model which includes models of the batteries and cables to the DC motor model is shown in Figure 2.6.

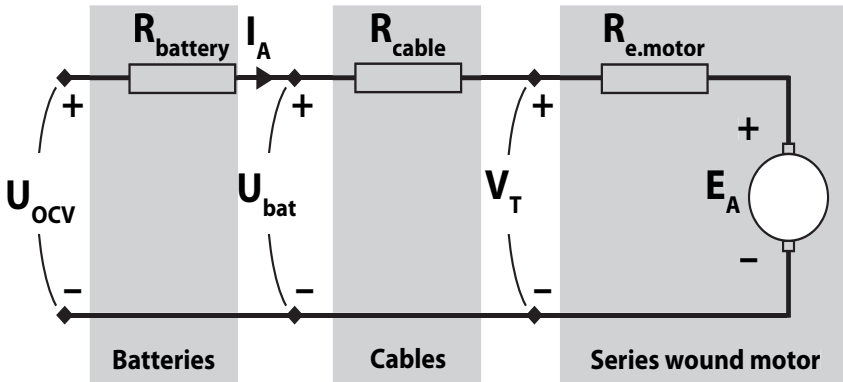


Figure 2.6. Complete circuit model for the starter motor system.

Here, U_{OCV} is the open circuit voltage, U_{bat} is the battery voltage, I_A the current in the system, V_T voltage over the starter motor and E_A is the armature voltage or back-emf. An expression for the relationship between current and speed is achieved by applying Equation (2.6) and Kirchoff's voltage law on the circuit in Figure 2.6.

$$I_A = \frac{U_{OCV}}{R_{battery} + R_{cable} + R_{e.motor} + KK_F \omega_m}. \quad (2.12)$$

Equation (2.12) highlights that it is possible to use a look up table to find the current by knowing the motor speed. This is a preferred solution for Scania instead of calculating the current.

2.2 Introduction To Heat Transfer

The basic relation of heat transfer between two mediums depend on temperature and heat flow. Temperature is stored energy and heat flow is thermal energy that moves from one medium to another. Both temperature and heat flow are effected by several material properties. The four most important ones are specific heat capacity, thermal conductivity, material density and mass [6].

2.2.1 Temperature and Heat Flow

The most commonly used equation for describing the heat flow rate, Q , from a body with temperature T is,

$$\frac{1}{C} Q(t) = \frac{d}{dt} T(t)$$

where C is the thermal capacity constant, which depends on the material and mass. The expression for the temperature as a function of the heat flow is then,

$$T(t) = \frac{1}{C} \int_0^t Q(s) ds + T(0). \quad (2.13)$$

2.2.2 Heat Transfer Modes

This section explains the three different types of heat transfer, *conduction*, *convection* and *radiation*. All three can occur either by themselves or in any combination.

Conduction

When thermal energy flows from higher temperature to lower temperature due to molecular contact in a medium or mediums in direct contact, this is called conduction. Fourier's law is the fundamental law of heat conduction and is given in Equation (2.14). The heat that flows through a material is proportional to the area through which the heat flows and to the negative temperature gradient [6],

$$q_{cond} = -k \frac{dT}{dx}. \quad (2.14)$$

Here, q_{cond} is the heat flux, T is temperature, k is thermal conductivity and x is the direction of the heat flow. In one-dimensional problems there is often no problem deciding which direction the heat should flow. A simple scalar form of Fourier's law is then used [6],

$$q_{cond} = -k \frac{\Delta T}{L},$$

where L is the length of the material in the direction of heat flow and q_{cond} and ΔT are both positive quantities. The total flow rate Q_{cond} is the heat flux multiplied by the area A , which gives,

$$Q_{cond} = q_{cond}A = -kA \frac{\Delta T}{L}.$$

Convection

Convection is the physical process of carrying heat away by a moving fluid. When cold air moves past a warm body, it sweeps away the warm air and replaces it with cold air, this is called convective cooling. The principle of convection is shown in Figure 2.7.

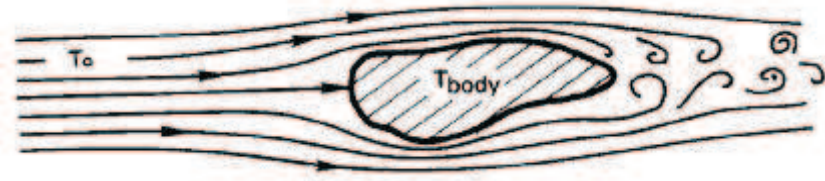


Figure 2.7. The principle of convection. When cold air moves past a warm body, it sweeps away the warm air and replaces it with cold air, this is called convective cooling [6].

The basic relationship for convected heat transfer is,

$$q_{conv} = h\Delta T, \quad (2.15)$$

where q_{conv} is the heat flux, ΔT is the temperature difference between the mediums and h is the heat transfer coefficient. Equation (2.15) is the steady-state form of Newton's law of cooling. The total heat flow rate, Q_{conv} , is calculated in a similar way as in conduction,

$$Q_{conv} = q_{conv}A = hA\Delta T,$$

where A is the contact area between the mediums [2].

Radiation

Radiation is the energy emitted from a body by electromagnetic radiation. The radiation intensity depends upon the temperature of the body and the nature of

its surface. Often the radiant heat transfer from cooler bodies can be neglected in comparison with conduction and convection [6]. The Stefan-Boltzmann law of a non-black body is,

$$e(T) = \epsilon\sigma T^4$$

where e is the energy flux, T is the temperature, $\sigma = 5.670400 \times 10^{-8} [W/m^2 K^2]$ is the Stefan-Boltzmann constant and ϵ is the emittance for the body. The emittance is, $\epsilon = 1$, for black bodies which are both perfect emitters and absorbers [6]. The heat transfer from a body is,

$$Q = e(T)A = \epsilon\sigma AT^4.$$

The transferred heat by radiation between two non-black bodies is,

$$Q_{net} = A_1 F_{1-2} (T_1^4 - T_2^4),$$

where F_{1-2} is the transfer factor, which depends on the emittance of both bodies as well as the geometrical view [9]. Heat transfer by radiation is proportional to the temperature to the power of four and σ is very small compared to conduction and convection for low temperatures [6]. Therefore the radiation will not be treated further in this report.

Overall Heat Transfer Coefficient

Heat is often transferred through series of different materials. Very often it is a combination of both conduction and convection. Due to low temperatures for the carbon brushes in a motor it is possible to neglect the radiation. It is then convenient to be able to describe the complete system with a constant, in this case U , which gives us

$$Q = UA\Delta T \tag{2.16}$$

where U is the overall heat transfer coefficient [6]. Equation (2.16) will be used in calculating the thermal load on the carbon brushes in Chapter 3.

Chapter 3

Modeling

3.1 Physical Description

Physical representations describing the heat transfer rate between the different parts in the starter motor area are in this chapter shown for both the Two State Model and the Single State Model. The arrows in Figure 3.2 and 3.3 illustrate the heat exchange between the different parts in the models. The representations are not ideal and every part of the systems can be further divided into smaller parts, but these models will hopefully suffice for the application at hand. Note that the effects of P_{loss} from Equation (2.11), which transfers heat to the carbon brushes during startup, is excluded in the pictures. The fastest temperature increase is in the brushes due to their small cross sectional area and the high passing currents. This thesis will focus on the carbon brushes and the windings temperature. In the next sections a software approach based on Figure 3.1 is used, where T_{out} , which is the outside temperature, and Engine Speed are input signals provided through available sensors on truck.

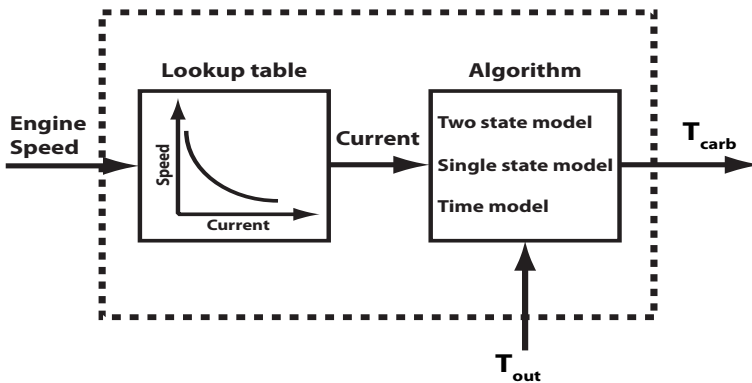


Figure 3.1. Overview of the software model for the estimation models, where T_{out} and Engine Speed are incoming signals provided through available sensors on truck.

Time Constrained Model

The simplest model for protecting the starter motor against overheating is a Time Constrained Model. This is the currently implemented overheating protection, allowing cranking for 35 seconds maximum with a 2 seconds cooling time. This model is introduced for comparison to the proposed state-space-model.

Single State Model

The physical description of the Single State Model is illustrated in Figure 3.2. This model is used to determine if one state is sufficient for protecting the starter motor against overheating. Here, T_{carb} is the current temperature in the positive brushes. Likewise, T_{out} indicates the temperature in the outside air and is available via temperature sensors on the truck. It is important to point out that these models are optimized for cranking the starter motor under very cold conditions. To reach high temperatures the starter motor must run on low speed, resulting in high currents flowing through the brushes. The load on the combustion engine increases with lower temperature because of friction in the engine and viscosity of the oil, resulting in high temperature increase in the brushes under freezing temperatures. Another way to reach low speed is to run the starter motor with a gear causing an increase in load and lowering in speed, but this user case is not considered.

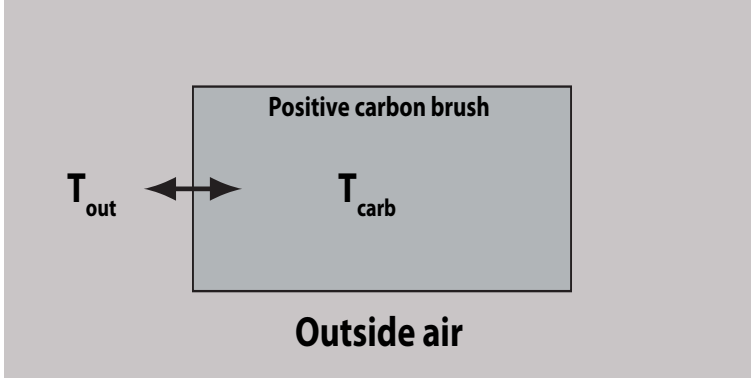


Figure 3.2. Single State Model for the starter motor carbon brushes

Using Equation (2.11) to model the heating,

$$P_{loss} = (R_A + R_F) I^2,$$

$$\dot{T} = \frac{P_{loss}}{c_p m_p} = \frac{(R_A + R_F)}{c_p m_p} I^2 = \theta_1 I^2,$$

where c_p is the thermal capacity constant, m_p the mass and θ_1 is a parameterized constant. Then Equation (2.16) is used to model the heat exchange between different mediums,

$$Q = UA\Delta T,$$

$$\dot{T} = \frac{Q}{c_p m_p} = \frac{UA}{c_p m_p} \Delta T = \theta_2 \Delta T,$$

where θ_2 is a parameterized constant. Then the continuous time-invariant equation for the Single State Model is

$$\dot{T}_{carb} = \theta_1 I^2 + \theta_2 (1 + \theta_3 \omega_m) (T_{out} - T_{carb})$$

$$\theta_i \geq 0, i = 1, 2, 3.$$

In the model, ω_m is the engine speed and is used as an added cooling factor. The extra cooling factor has only a minor impact on the heat exchange, but is assumed to be speed dependent and should represent the effect from the airflow through the starter motor. The parameters that needs to be calibrated are θ_i , $i = 1, 2, 3$.

Two State Model

The Two State Model model includes two states, T_{carb} (positive carbon brush) and T_{wind} (windings). The model input T_{out} is the outside temperature and is available via temperature sensors on the truck. The two states were chosen based on temperature observations during initial tests performed on truck. Figure 3.3 illustrates the relationship between the different parts.

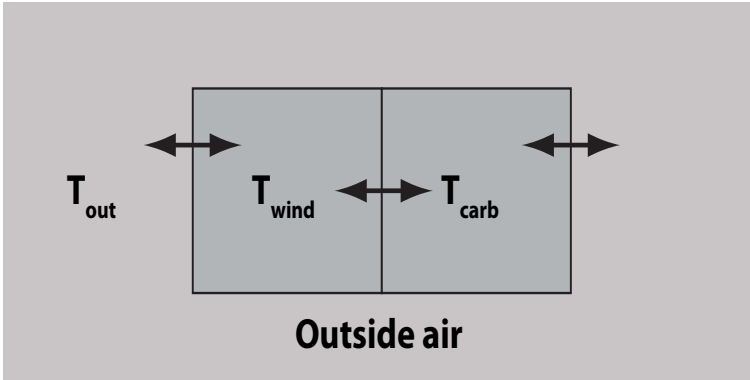


Figure 3.3. Two State Model for the starter motor positive carbon brush

Using the same theory as for the Single State Model, the continuous time-invariant equations for the Two State Model are

$$\dot{T}_{carb} = \theta_1 I^2 + \theta_2 (T_{wind} - T_{carb}) + \theta_3 (1 + \theta_4 \omega_m) (T_{out} - T_{carb})$$

$$\dot{T}_{wind} = \theta_5 I^2 + \theta_6 (T_{carb} - T_{wind}) + \theta_7 (1 + \theta_8 \omega_m) (T_{out} - T_{wind})$$

$$\theta_i \geq 0, i = 1, 2, \dots, 8.$$

In the model, ω_m is the engine speed and is used as an added cooling factor. The extra cooling factor has only a minor impact on the heat exchange, but is assumed to be speed dependent and should represent the effect from the airflow through the starter motor. The parameters that needs to be calibrated are θ_i , $i = 1, 2, \dots, 8$.

3.2 Warm Up

Information from the starter motor manufacturer shows that the highest temperature in a starter motor is in the positive brush [4]. The overheating in a starter motor is caused by high currents floating through small carbon brushes. This implies that the warm up is dominated by the current, $\theta_i I^2$. When the carbon brushes reach temperatures over 325° Celsius the brushes are damaged [4].

3.3 Parameter Calibrations

For calibrating the different tuning parameters in the models the gray box method is used. This means that there is knowledge about the internal structure of the system, in this thesis the physical properties. To be able to calibrate the different tuning parameters in the models the input data, which are the current, engine speed and outside temperature, and output data, which is the temperature in the positive brush, are available and shown in Figure 3.4 and Figure 3.5. The tuning parameters in the different models are calibrated using the input and output data from a first test and then validated with the input data against the output data in a second test. The first test has two cranking periods and the second has five cranking periods. The parameters are tuned between $T_{carb,max} = 325^\circ$ Celsius and $T_{carb} = 100^\circ$ Celsius, which are chosen as the maximum allowed temperature and the minimum reached temperature before allowing start after overheating has occurred. The minimum temperature can be chosen differently, but is set to a specific value by Scania so that the waiting time is under approximately 15 minutes before a new starting attempt is allowed, but the methodology is generic. This implementation method with a waiting time after an overheating has occurred is decided by Scania. You dont want high temperatures in the brushes, by using a waiting time, the temperature drops to a lower level before a new starting attempt is allowed, thus minimizing the time with critical temperatures.

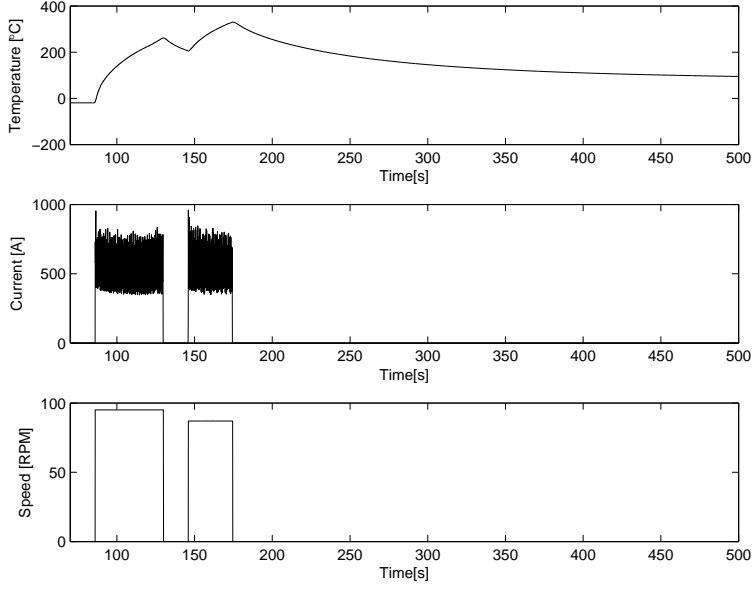


Figure 3.4. Measured signals used for parametrization of the models. First plot shows the measured temperature in the positive brush, the second plot shows the measured current to the starter motor and the third plot shows the measured engine speed.

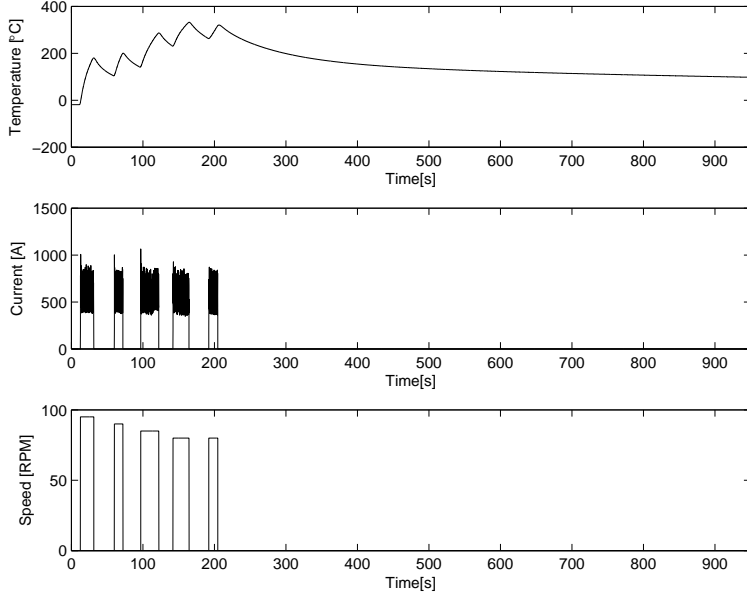


Figure 3.5. Measured signals used for verification of the models. First plot shows the measured temperature in the positive brush, the second plot shows the measured current to the starter motor and the third plot shows the measured engine speed.

Chapter 4

Results and Discussion

The temperature for the positive brush in the starter motor was the focus during all testing. The fastest temperature increase is in the brushes due to their small cross sectional area and the high currents passing through them during low engine speed. The test setup which was used for gathering all data is shown in Figure 4.1. The measured signals were voltage over the starter motor and the batteries, starter motor current, outside temperature, engine speed and different starter motor temperatures. Both outside temperature and engine speed are available through the CAN bus, which is located on truck.

4.1 Testing and Verification

Initial testing were performed in a temperature at roughly 10° Celsius, but these tests were not usable due to problems in reaching high temperatures in the starter motor brushes. To stress the brushes long enough to reach critical temperatures, healthy batteries were needed, but even these were not a guarantee. During the tests it was clear that the problem for the starter motor was the voltage drop between the batteries and the motor, not the temperature in the brushes. The voltage drop lowers the output effect of the starter motor, thus making it harder for the engine to start. The usable tests were performed under -20° Celsius and additional batteries were used to increase the cranking time during the tests. To prevent the engine from starting, the fuel injectors were closed. The truck used in testing was a 13 liter 6-cylinder diesel engine. The starter motor was a Bosch HXF95L-24V with an output power of maximum 6.5 kW [4]. For parameterization of the models, both the Single and the Two State Model are fed with the current from the second plot in Figure 4.2 and the engine speed from the first plot in Figure 4.4. For verification of the models, both the Single and the Two State Model are fed with the current from the second plot in Figure 4.3 and the engine speed from the second plot in Figure 4.4. The outside temperature is set to -20° Celsius.

4.1.1 Complete Test on Truck

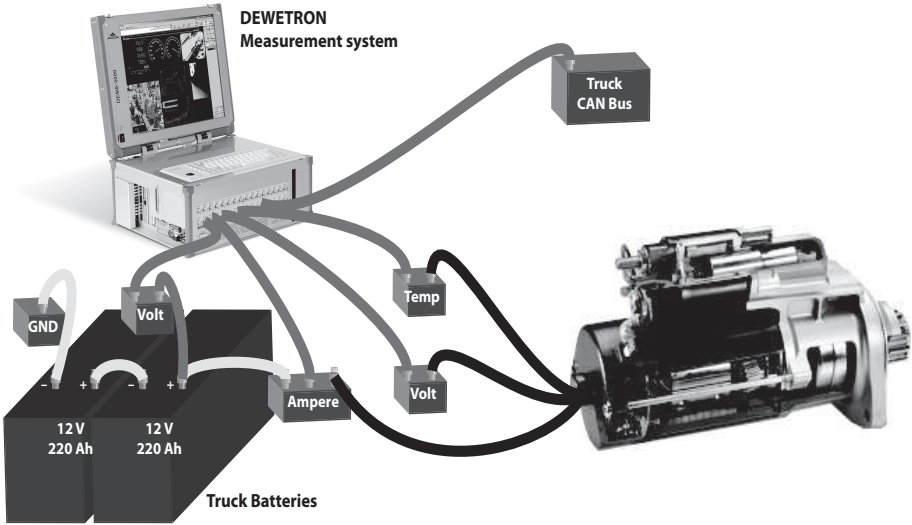


Figure 4.1. Test setup on truck. The Dewetron system is used for logging all data.

A test case with two cranking periods was performed for parametrization of the models. First plot in Figure 4.2 illustrates the data from the test. All temperatures started under -20° Celsius. The second plot in Figure 4.2 illustrates the input signal which is later used for parameterization. The large variations in the current are caused by the cylinders combustions in the engine, which causes the engine speed to vary, causing the current to vary. High currents run through small brushes in the starter motor, which results in a large increase of the brush temperature.

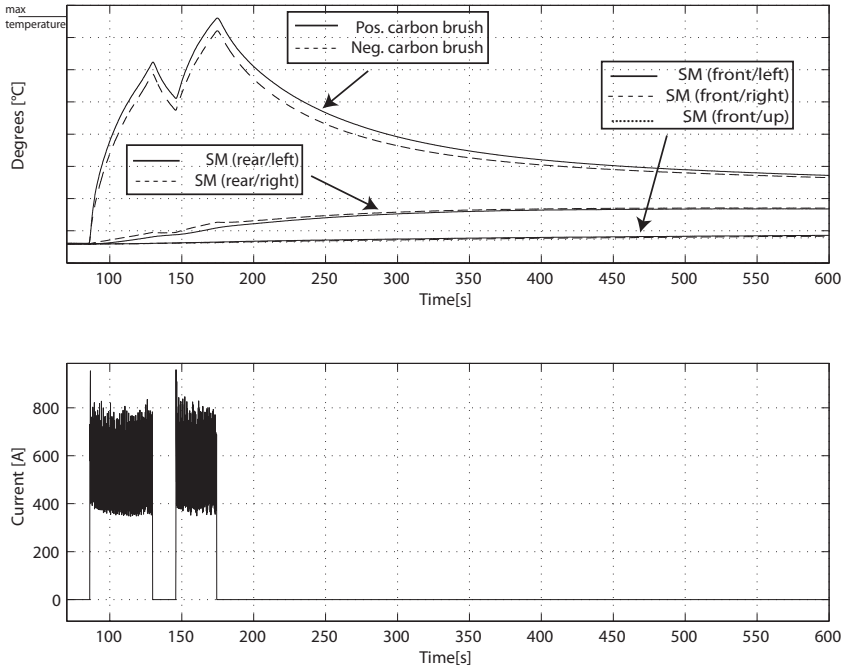


Figure 4.2. First plot is a test on truck used for parametrization of the models. SM stands for Starter Motor goods and is combined with the positions of the temperature sensors. The rear sensors are placed close to the brush sensors, which also are located at the rear. First cranking time lasts for 44 seconds followed by a 16 seconds waiting time. Second cranking time lasts for 28 seconds. The second plot shows the measured current from the test on the truck. The large variations in the measured current are caused by the cylinders combustions in the engine, which causes the engine speed to vary, causing the current to vary. This signal is used as input signal for the models.

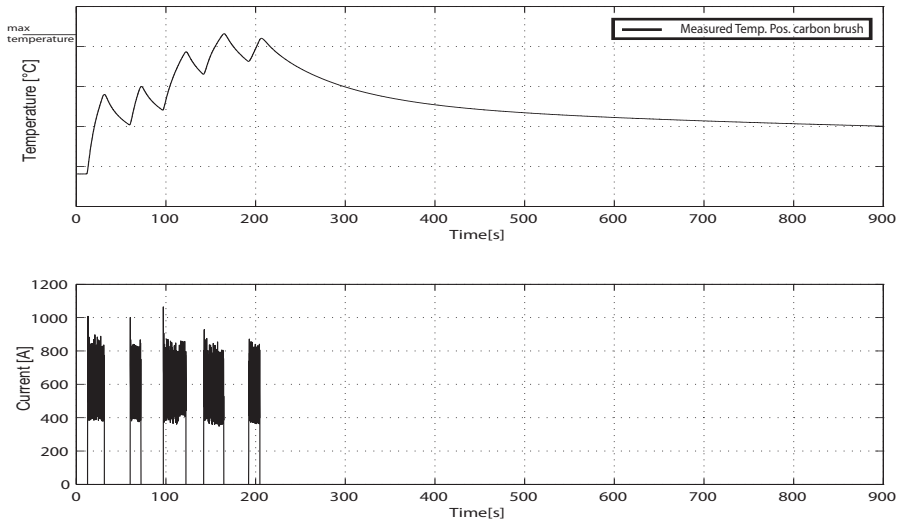


Figure 4.3. First plot is a test on truck used for verification of the models. The cranking and cooling sequences are; 19 seconds of cranking, 29 seconds of cooling, 13 sec. crank., 24 sec. cool., 26 sec. crank., 19 sec. cool., 23 sec. crank., 27 sec. cool. and 15 sec. crank.. The second plot shows the measured current from the test on the truck. The large variations in the measured current are caused by the cylinders combustions in the engine, which causes the engine speed to vary, causing the current to vary. This signal is used as input signal for the models.

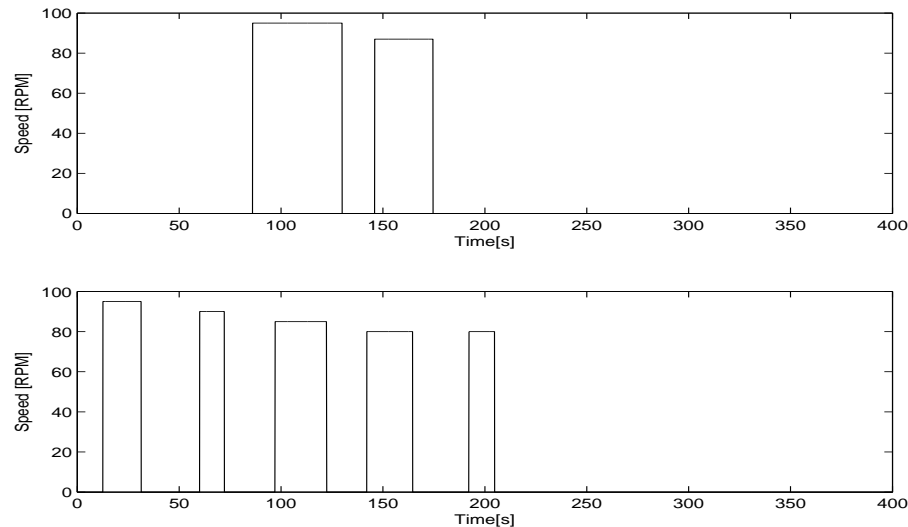


Figure 4.4. The first plot shows the engine speed during the first test. The second plot shows the engine speed during the second test. The engine speed signal is low pass filtered before presented on the CAN bus. These signals are used as input signals for the models.

4.1.2 Time Constrained Model

A time constrain algorithm is already available and implemented in production trucks. This section shows the drawbacks of a Time Constrained Model instead of a State Model. Figure 4.5 shows the temperature in the positive brush when the starter motor has a 35 seconds cranking time followed by 2 seconds of cooling and then another 35 seconds of cranking. This type of cranking will overheat the starter motor and cause the brushes to be damaged, possibly destroyed. This behavior is allowed with the current implementation.

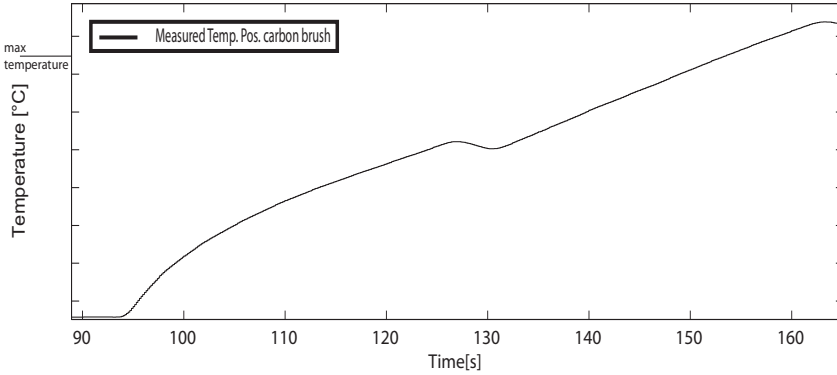


Figure 4.5. The result of cranking the starter motor for 35 seconds followed by 2 seconds cooling and another 35 seconds cranking. During this test the brush temperature reaches approximately $1.14 \times \text{max. temperature}$, which makes the brushes to burn out.

4.1.3 Single State Model

The Single State Model from Chapter 3 is parameterized and evaluated in this section. Note that the model is optimized when $100^{\circ}\text{C} \leq T_{carb} \leq 325^{\circ}\text{C}$, that is why the model is poor during cooling and drops fast to the outside temperature. Figure 4.6 shows the result of the parameterized model based on the current presented in the second plot in Figure 4.2 and the engine speed presented in the first plot in Figure 4.4. The outside temperature during the tests is -20°C . It is possible to get a good accuracy during temperature rise, but during cooling the negative effects of using a Single State Models is very clear. Without a second state that can hold up the temperature during cooling, the modeled brush temperature will quickly drop to the outside temperature.

A second test is performed for verification with multiple starts, the result is shown in Figure 4.7. The cranking and cooling sequences are; 19 seconds of cranking, 29 seconds of cooling, 13 sec. crank., 24 sec. cool., 26 sec. crank., 19 sec. cool., 23 sec. crank., 27 sec. cool. and 15 sec. crank.. During this test, without fresh batteries, it is most likely that the batteries will be drained before the overheating occurs.

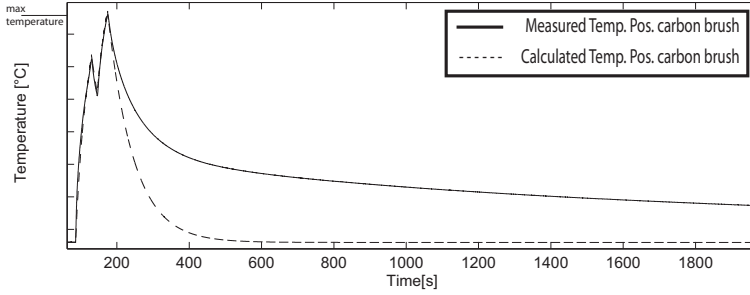


Figure 4.6. Calibrated Single State Model. First cranking time lasts for 44 seconds followed by a 16 seconds waiting time period. Second cranking time lasts for 28 seconds. A zoomed version is available in Figure A.2 in appendix.

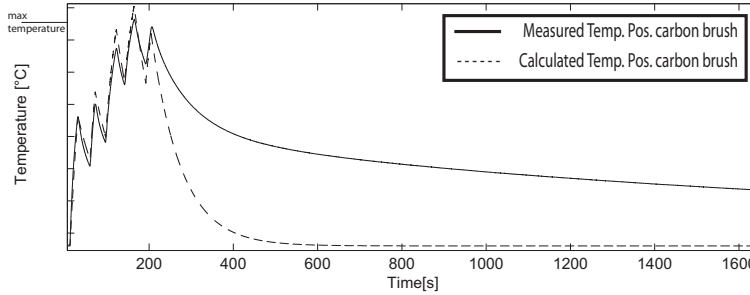


Figure 4.7. Single State Model verification. The accuracy is better than the Two State Model during heating, but not close to the the Two State Model during cooling. A zoomed version is available in Figure A.3 in appendix.

4.1.4 Two State Model

The result from the adapted algorithm for the Two State Model is shown in Figure 4.8. The signals presented in Figure 4.2 are used for parameterizing the algorithm. The estimated temperature is very close to the measured temperature under heating with only a small mismatch. During cooling there is a larger, but still small, mismatch between the measured temperature and the estimated temperature.

A second test is performed for verification with multiple start attempts and the same parameters as in the algorithm in Figure 4.8. The result is shown in Figure 4.9. The cranking and cooling sequences are the same as for the Single State Model. During normal conditions, and without fresh batteries, it is most likely that the batteries will be drained before the overheating occurs.

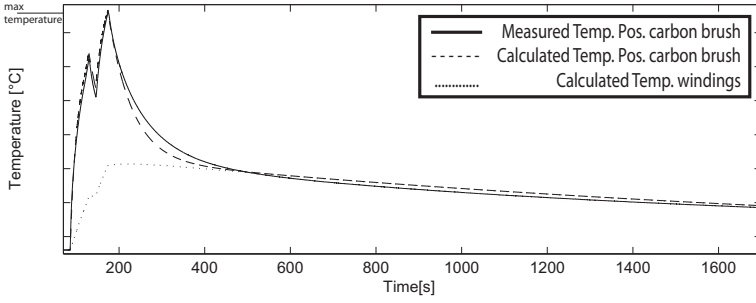


Figure 4.8. Testing of the calibrated Two State Model. First cranking time lasts for 44 seconds followed by a 16 seconds waiting time. Second cranking time lasts for 28 seconds. A zoomed version is available in Figure A.4 in appendix.

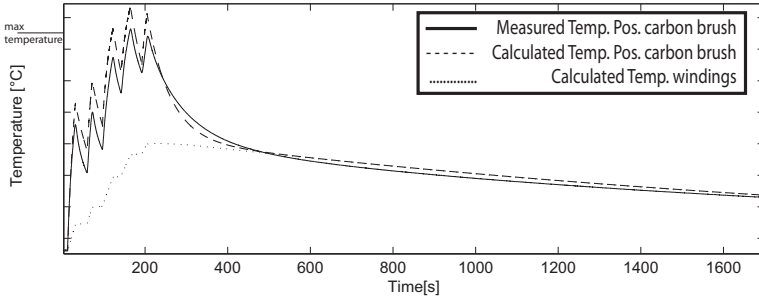


Figure 4.9. Verification with multiple cranking intervals for the Two State Model. The algorithm is overestimating the brush temperature, which is positive. During this test extra batteries were needed to be able to repeatedly crank the starter motor. A zoomed version is available in Figure A.5 in appendix.

4.1.5 Waiting Time Estimation

To be able to present, for the truck driver, a waiting time after an overheating has occurred, a model of estimating the waiting time is needed. Instead of simulating the Two State Model to find the needed time to reach a specific value, which puts high loads on the CPU, another method is chosen which spreads the calculations over time. With this model the accuracy is improved with every time step, but you can also choose how often and not update the estimated waiting time with every time step. The derivation of the final expression can be read about in appendix,

$$t_{wait} = \frac{1}{k_{tot}} \ln \left(\frac{\frac{\alpha T_{carb}(t_{start}) + T_{wind}(t_{start})}{1+\alpha} - T_{amb}}{T_{100} - T_{amb}} \right) \quad (4.1)$$

where t_{wait} is the estimated time to reach the temperature T_{100} . This model is used for estimating the waiting time when overheating has occurred. The results, when the model is applied on the Two State Model, are shown in Figure 4.10 and

Figure 4.11. The estimated waiting time performs almost perfect compared to the true waiting time for the calculated brush.

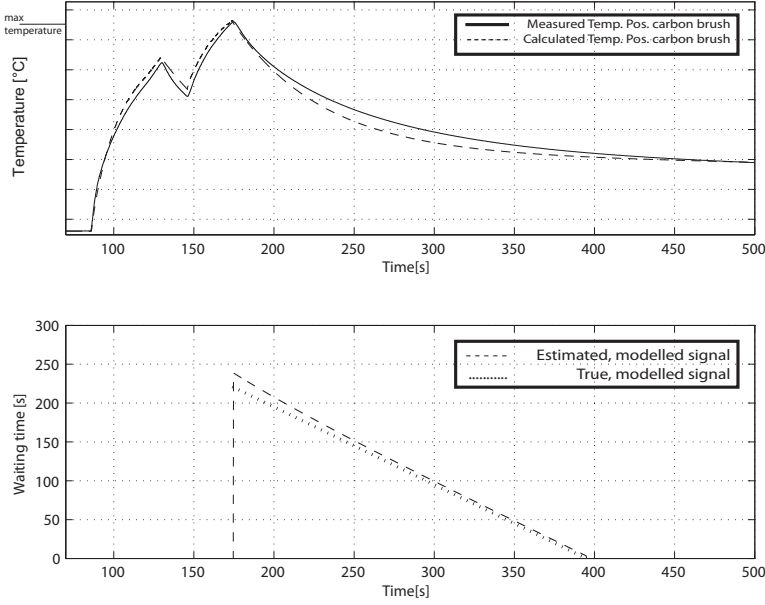


Figure 4.10. First plot is from Figure 4.8. The second plot shows the different waiting times. Estimate, modeled signal, are calculated through Equation (4.1). The true waiting time are the needed waiting time for the measured brush to reach T_{100} .

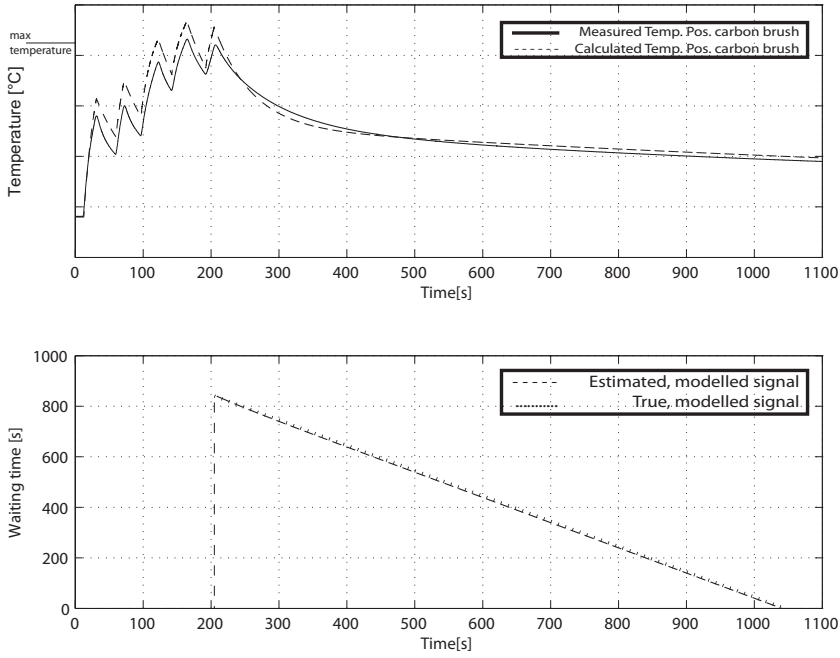


Figure 4.11. First plot is from Figure 4.9. The second plot shows the different waiting times. Estimate, modeled signal, are calculated through Equation (4.1). The true waiting time are the needed waiting time for the measured brush to reach T_{100} .

4.2 Discussion

Comparing the Two State Model from Figure 4.8 and Single State Model from Figure 4.6 clearly illustrates the gain of adding a second state to the model. The second state, T_{wind} , in the Two State Model makes the first state, T_{carb} , stay on a higher level instead of dropping to the outside temperature like in the Single State Model. The Time Constrained Model shows poor performance when the engine speed is low resulting in high currents. This is clearly shown in Figure 4.5. It is possible to add more states to the Two State Model to reach better performance, but the result will be a system with a great complexity and is more time consuming for parameterization. When implementing a model executing in real time on truck, there may be a need of recalibrating parameters, due to possible mismatches from the lookup table for converting engine speed to current. It may also be that the lookup table also needs to be recalibrated. The model for waiting time estimation shows good performance in both the two starts test and multiple starts test.

Software Architecture

A possible software architecture for the implementation of the algorithm is presented in Figure 4.12. This is presented as a possible solution. When or if the model will be implemented, the implementer will be responsible for choosing a suitable software architecture. The state machine keeps track of when the starter motor is overheated. The main program handles the start-up process, first checking for incoming start requests and then checks if a gear is engaged, due to have the possibility to move the truck with the starter motor in an emergency.

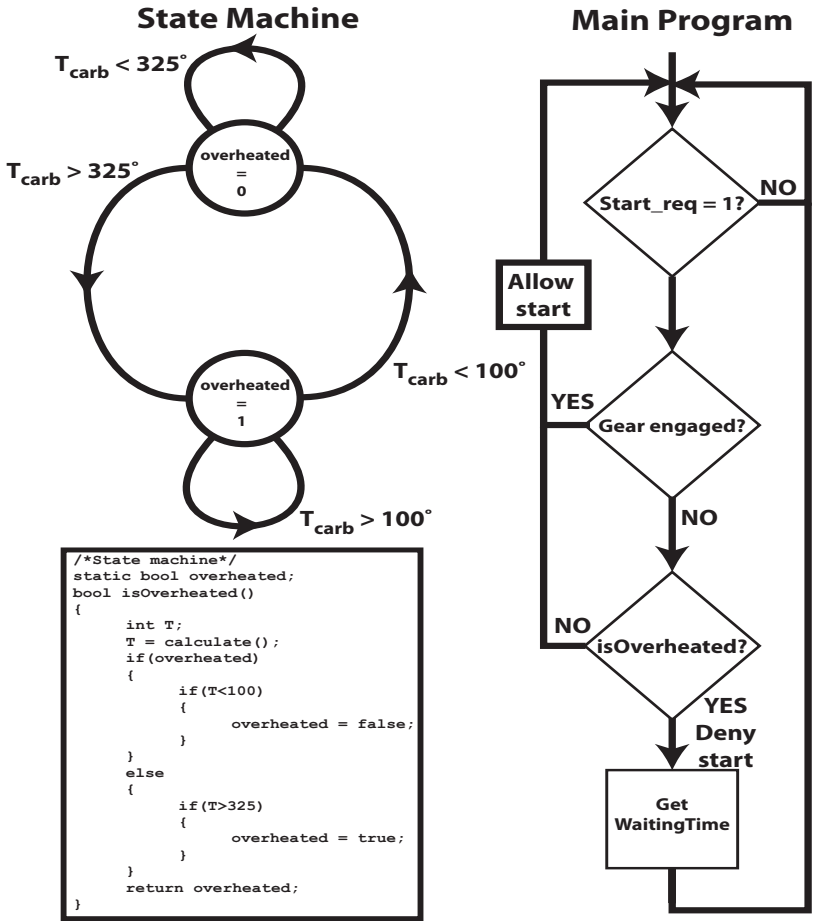


Figure 4.12. State Machine with Main Program

Chapter 5

Conclusions and Future Work

5.1 Conclusions

An implementation of the calibrated Two State Model is recommended. The model is not complex and a calibration of the model on truck with available input signals is feasible. A lookup table, provided by the motor manufacturer, for converting the speed to current should also be implemented. A suggested software architecture is presented in Figure 4.12. Another focus from Scania would be to handle the voltage drop, from cables, between the batteries and the starter motor. This would improve the performance of the starter motor, thus lowering the temperature in the brushes.

5.2 Future Work

The next step is to make a software implementation on truck. Tests prove that with the Two State Model it is possible to make a protection that is effective enough to protect the starter motor and at the same time maximizes the cranking time. The model's parameters must probably be reconfigured once the algorithm is implemented on truck.

An added feature in the future would be to save data like, low speed runtime and total runtime, for detecting the lifespan for a specific starter motor. This can be used to predict that a starter motor needs to be replaced, before it brakes down.

The -20° Celsius tests showed that the batteries could not run the starter motor long enough to reach high temperatures in the brushes. This is believed to be caused by the voltage drop from R_{cable} between the batteries and the starter motor in Figure 2.6. This causes the starter motor to run in an interval it is not optimized for. To be able to supply the starter motor with enough current, fresh batteries were needed. It was obvious that the voltage drop between the starter motor and the batteries was high enough to sometimes prevent the engine to start

during low temperatures. A strong recommendation is to find a way to minimize this voltage drop. This will further protect the starter motor and also greatly improve the start performance of the engine.

Bibliography

- [1] Walter N. Alerich and Jeff Keljik. *Electricity 4: AC/DC Motors, Controls, and Maintenance*. Thomson Learning, 7th edition, 2001.
- [2] Adrian Bejan and Allan D. Kraus. *Heat transfer handbook*. John Wiley and Sons, 2003.
- [3] James H. Bentley and Hesham E. Shaalan. *Electrical Engineering: A Referenced Review*. Kaplan AEC Education, 4th edition, 2005.
- [4] Bosch. *Dialog with the starter motor manufacturer*. Bosch, 2009.
- [5] Allan R. Hambley. *Electrical Engineering, Principles and Applications*. Pearson Education, Inc., 4th edition, 2008.
- [6] John H. Lienhard IV and John H. Lienhard V. *A Heat Transfer Textbook*. Phlogiston Press Cambridge, Massachusetts, U.S.A., 3rd edition, 2008. URL: <http://web.mit.edu/lienhard/www/ahtt.html>.
- [7] MAN. *Drivers Manual*. Truck Manufacturer, 2009.
- [8] Mercedes. *Drivers Manual*. Truck Manufacturer, 2009.
- [9] Tariq Muneer, Jorge Kubie, and Thomas Grassie. *Heat transfer: a problem solving approach*. Taylor and Francis, 2003.
- [10] Spark Museum. *The Development of the Electric Motor*. Spark Museum, 2010. URL: <http://www.sparkmuseum.com/MOTORS.HTM>.
- [11] Carl Nordling and Jonny Österman. *Physics Handbook: for Science and Engineering*. Studentlitteratur, 6th edition, 1999.
- [12] Volvo. *Drivers Manual*. Truck Manufacturer, 2009.

Appendix A

Appendix

A.1 Time Estimation

To find a good estimation for the waiting time a few assumptions are made. Figure A.1 illustrates these assumptions, $T_{tot}(t)$ and $E_{tot}(t)$ represent the average temperature and the total energy for the brush and windings. Both $T_{tot}(t)$ and

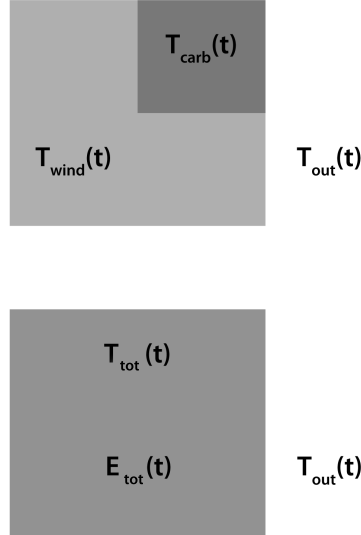


Figure A.1. Graphical interpretation for waiting time estimation. $T_{tot}(t)$ represent the average temperature for the brush and the windings. $E_{tot}(t)$ represent the total energy for the brush and the windings.

$E_{tot}(t)$ are represented by the following equations.

$$\begin{aligned} T_{tot}(t) &= \frac{E_{tot}(t)}{m_{tot}c_{p,tot}} \\ E_{tot}(t) &= m_{carb}c_{p,carb}T_{carb}(t) + m_{wind}c_{p,wind}T_{wind}(t) \\ \dot{T}_{tot}(t) &= k_{tot}(T_{amb} - T_{tot}(t)) \end{aligned}$$

Now $E_{tot}(t)$ is simplified by the following expressions,

$$\begin{aligned} m_{carb}c_{p,carb} &= k_{carb} \\ m_{wind}c_{p,wind} &= k_{wind} \end{aligned}$$

resulting in

$$E_{tot}(t) = k_{carb}T_{carb}(t) + k_{wind}T_{wind}(t). \quad (\text{A.1})$$

Of course the following expression is true,

$$m_{tot}c_{p,tot} = m_{carb}c_{p,carb} + m_{wind}c_{p,wind} = k_{carb} + k_{wind}. \quad (\text{A.2})$$

Equation (A.1) and Equation (A.2) are now used in $T_{tot}(t)$

$$T_{tot}(t) = \frac{E_{tot}(t)}{m_{tot}c_{p,tot}} = \frac{k_{carb}T_{carb}(t) + k_{wind}T_{wind}(t)}{k_{carb} + k_{wind}}$$

Now $T_{tot}(t)$ is simplified by the following expressions,

$$\alpha = \frac{k_{carb}}{k_{wind}}$$

resulting in

$$T_{tot}(t) = \frac{\alpha T_{carb}(t) + T_{wind}(t)}{1 + \alpha}.$$

The heat transfer between $T_{tot}(t)$ and T_{amb} is

$$\dot{T}_{tot}(t) = k_{tot}(T_{amb} - T_{tot}(t)).$$

Resulting in the differential equation,

$$\dot{T}_{tot}(t) + k_{tot}T_{tot}(t) = k_{tot}T_{amb}.$$

The solution for the homogeneous equation,

$$T_{tot,h}(t) = C_{tot}e^{-k_{tot}t}.$$

The solution for the particular integral,

$$T_{tot,p}(t) = T_{amb}.$$

The expression for $T_{tot}(t)$ is the sum of the homogeneous equation and particular integral,

$$T_{tot}(t) = C_{tot}e^{-k_{tot}t} + T_{amb}.$$

Inserting $t = t_{start} = 0$ to find C_{tot} ,

$$T_{tot}(t_{start}) = C_{tot} + T_{amb} = \frac{\alpha T_{carb}(t_{start}) + T_{wind}(t_{start})}{1 + \alpha}$$

which ends in,

$$C_{tot} = \frac{\alpha T_{carb}(t_{start}) + T_{wind}(t_{start})}{1 + \alpha} - T_{amb}.$$

The final expression for $T_{tot}(t)$ is,

$$T_{tot}(t) = \left(\frac{\alpha T_{carb}(t_{start}) + T_{wind}(t_{start})}{1 + \alpha} - T_{amb} \right) e^{-k_{tot}t} + T_{amb}. \quad (A.3)$$

Now to find the waiting time until the starter motor may be used again, $t = t_{wait}$ is inserted in Equation (A.3),

$$T_{tot}(t_{wait}) = \left(\frac{\alpha T_{carb}(t_{start}) + T_{wind}(t_{start})}{1 + \alpha} - T_{amb} \right) e^{-k_{tot}t_{wait}} + T_{amb}.$$

The final expression for estimating the waiting time when $T_{tot}(t_{wait}) = T_{100}$ is,

$$t_{wait} = \frac{1}{k_{tot}} \ln \left(\frac{\frac{\alpha T_{carb}(t_{start}) + T_{wind}(t_{start})}{1 + \alpha} - T_{amb}}{T_{100} - T_{amb}} \right). \quad (A.4)$$

Here, T_{100} is the temperature when a new start is allowed.

A.2 Zoomed Plots

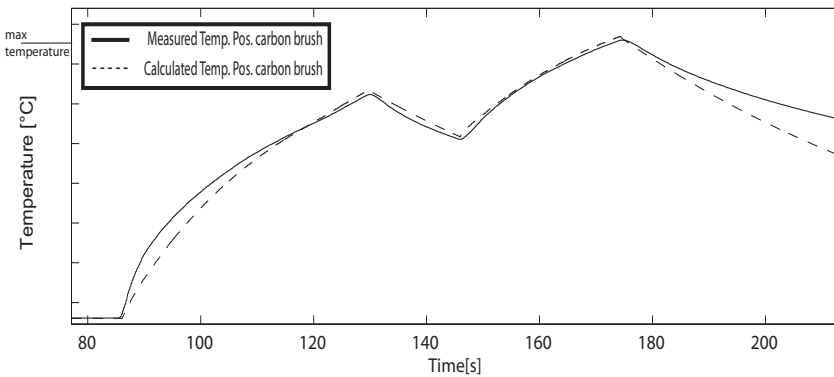


Figure A.2. Calibrated Single State Model testing. Zoomed version of Figure 4.6. First cranking time lasts for 44 seconds followed by a 16 seconds waiting time. Second cranking time lasts for 28 seconds.

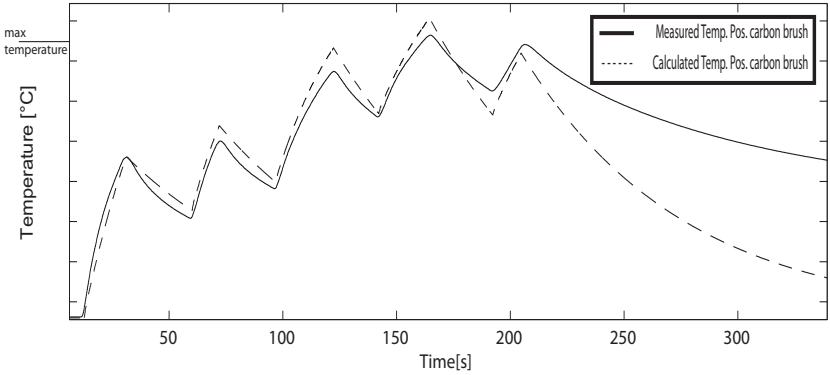


Figure A.3. Single State Model verification. Zoomed version of Figure 4.7.

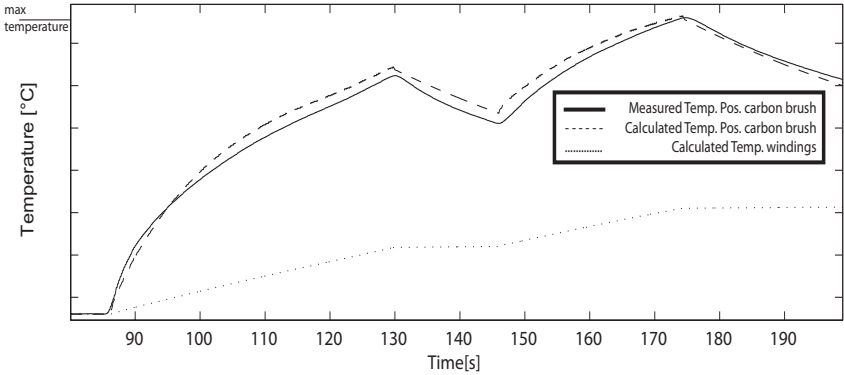


Figure A.4. Calibrated Two State Model testing. Zoomed version of Figure 4.8. First cranking time lasts for 44 seconds followed by a 16 seconds waiting time. Second cranking time lasts for 28 seconds.

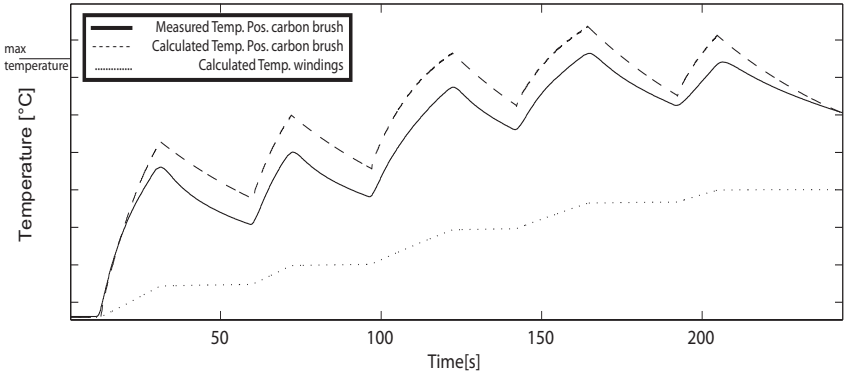


Figure A.5. Two State Model verification. Zoomed version of Figure 4.9.